A PCB Integrated Differential Rogowski Coil for Non-Intrusive Current Measurement Featuring High Bandwidth and dv/dt Immunity

Jan Niklas Fritz, Christoph Neeb and Rik W. De Doncker
Institute for Power Electronics and Electrical Drives, RWTH Aachen University
Jaegerstr. 17/19, 52066 Aachen, Germany
Email: post@isea.rwth-aachen.de

***Abstract*—In the development of next-generation power modules for electric vehicles, demands for high efficiency, reliability, low cost, high power density and therefore small size are of major importance. A promising approach is the embedding of power semiconductor devices into a printed circuit board (PCB), as investigated by the *HI-LEVEL* project.**

This paper deals with the research, design and experimental verification of a current sensor based on the principle of a Rogowski coil, which is integrated into a PCB, so that it can measure the device current of the embedded power semiconductor devices. As switched-mode currents are to be measured, the dynamics of the current sensor were of major concern. Moreover, as large voltage gradients caused by the semiconductor devices inject parasitic capacitive currents into the coil, a differential measurement approach was selected for cancelling out disturbances caused by capacitive coupling.

***Index Terms*—Rogowski coil, current sensor, differential Rogowski coil, PCB, capacitive coupling, HI-LEVEL**

I. Introduction

Power electronics are indispensable for the development of next-generation hybrid and fully electric vehicles. Apart from mandatory claims for high efficiency, high reliability and low cost, also the demand for little installation space and therefore higher power density becomes increasingly important [11]. As a promising approach, the *HI-LEVEL* project, which is financed by the *German Federal Ministry of Education and Research*, investigates the advantages of embedding power semiconductor devices into PCBs [11, 16]:

- The total volume is reduced, offering the possibility to mount the system directly at the electric machine and to increase power density.
- Electric lengths are shortened, which reduces stray inductance and overvoltages during turn-off. Therefore, the system can be operated at higher voltage than usually, which increases transferred power and power density. Additionally, switching losses are minimized.
- Due to the reduction in complexity of the setup, the cost of the manufacturing processes can be minimized.
- As packaging is prone to mechanical and thermal stress, it is a common reason for a power electronic system's failure. PCB integration increases reliability and monitoring circuitry can be placed on the PCB instead.

Said implementation of monitoring circuitry was the idea motivating this paper, which deals with the development of a current sensor for measuring the device current of the power semiconductors. The main requirement was to maintain the advantages of the embedding technique. In order to keep electric lengths short, the current sensor had to be integrated into the PCB as well. Additionally, the low stray inductance in the switching path forbade the use of an iron core.

Instead, the principle of a Rogowski coil was chosen. It is known since 1887, when A. P. Chattock developed a measuring method for the magnetic voltage [1], which is defined the line integral of the magnetic field strength $\overrightarrow{H}$. If such a voltage is measured along a closed contour C, the Maxwell-Ampère equation in quasi-stationary approximation

$$\oint_C \overrightarrow{H} \cdot \mathrm{d}\overrightarrow{s} \approx I_{\mathrm{enclosed}} \tag{1}$$

states that it will be proportional to the enclosed current. In 1912, W. Rogowski and W. Steinhaus [2] proposed an apparatus quite similar to Chattock's coil and reported current measurements using the new device. Since then, this device has been called *'Rogowski coil'*. A main advantage is that the absence of ferromagnetic material eliminates nonlinearities and hysteresis effects [9, 10]. But because of the low output voltage and the need for additional integrator circuitry, see section III-C, first the development of modern signal processing and integrated circuits promoted the use of Rogowski coils [10]. Integration of Rogowski coils into PCBs has widely been reported in literature.

The following sections will discuss the theory of Rogowski coils, the design process of a prototype PCB and the experimental results that could be achieved with the PCB Rogowski coil after some improvement steps.

II. Theory of operation

A. Coil model

In figure 1, a sketch of a Rogowski coil is shown. According to (1), the current $i_1(t)$ causes a magnetic field strength $\overrightarrow{H}(t)$ and, because of the absence of ferromagnetic material, a flux density $\overrightarrow{B}(t) = \mu_0 \overrightarrow{H}(t)$ penetrating the turns. Because of the Maxwell-Faraday equation

$$\oint_C \overrightarrow{E} \cdot \mathrm{d}\overrightarrow{s} = -\frac{\mathrm{d}}{\mathrm{d}t} \iint_A \overrightarrow{B} \cdot \mathrm{d}\overrightarrow{A} = -\frac{\mathrm{d}\phi}{\mathrm{d}t}, \tag{2}$$

a voltage is induced between the ends of the coil that is proportional to the time derivative of $i_1(t)$. By integrating the coil voltage, finally the current $i_1(t)$ can be obtained.

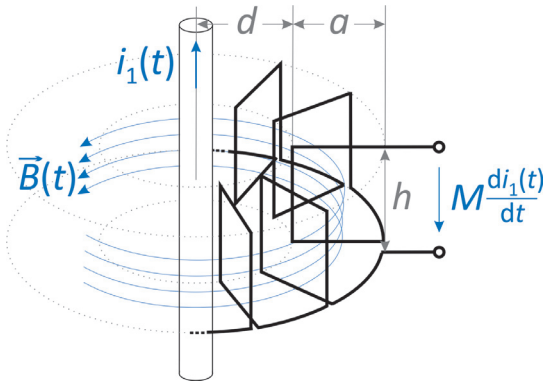

Figure 1: Sketch of a Rogowski coil.

In figure 2, an electrical model of a Rogowski coil is displayed [5, 7, 9, 13]. The mutual inductance M of the setup determines the magnitude of the induced voltage, which is modelled as a voltage source

$$u_{\mathrm{ind}}(t) = -M\frac{\mathrm{d}i_1(t)}{\mathrm{d}t} \ . \tag{3}$$

Additionally, the ohmic resistance R_s and the self-inductance L_s of the winding are added to the model. Between the turns of the coil, there would be also parasitic capacitances, which are considered as a lumped element C_s for simplification. Apart from the mutual inductance M, also the self-inductance L_s and the self-capacitance C_s are of major importance in coil design, as their resonance frequency limits the bandwidth of the coil and therefore the dynamics of the whole measurement. Today, the bandwidth of commercial Rogowski coils ranges up to tens of MHz (with integrator) [15]. Finally, an external resistor is included in the model, which should be used to damp said resonances.

From electromagnetic field calculation, the mutual inductance M and the self-inductance L_s of the coil geometry that is depicted in figure 1, assuming N rectangular turns and rotational symmetry, can be calculated [3]:

$$M = \mu_0\frac{Nh}{2\pi}\log\left(1+\frac{a}{d}\right) \tag{4}$$

$$L_\mathrm{s} = N \cdot M \tag{5}$$

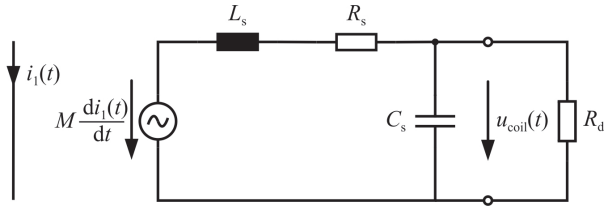

Figure 2: Equivalent circuit of a Rogowski coil, valid up to the first resonance frequency.

B. Design considerations

The measurement accuracy of a Rogowski coil is limited by dynamics on the one hand and a finite number of turns N on the other hand. With increasing number of turns, the self-inductance L_s rises faster than M according to (5) and therefore the resonance frequency drops.

But a high number of turns is desirable as it increases measurement accuracy [3]: The MAXWELL-AMPÈRE law (1) states that $\frac{\mathrm{d}i_1(t)}{\mathrm{d}t}$ is proportional to the time derivative of the line integral of the magnetic field strength. However, the voltage induced in each (discrete) turn is added, which would be represented by a sum, not a line integral. Hence, a Rogowski coil performs a RIEMANN approximation of the said line integral and therefore, only an approximation of $\frac{\mathrm{d}i_1(t)}{\mathrm{d}t}$. In ROGOWSKI's original publication [2], he discusses this issue and consequently recommends a high number of turns.

With PCB integrated Rogowski coils, the tradeoff between dynamics and accuracy can be relieved by utilizing the main advantage of PCB integration – that the whole setup is fixed. In theory, the design of a rotational symmetric coil, with the current exactly centered in its mid, causes the magnetic field to be constant at each angle. Then the RIEMANN approximation would be satisfactory even for a low number of turns, which would guarantee good dynamic performance.

III. SYSTEM DESIGN

A. 4-layer PCB layout

A prototype of the projected Rogowski coil was set up on a standard 4-layer PCB. In order to achieve similar conditions as in the *HI-LEVEL* PCB, a half bridge of two *BSC028N06NS* MOSFETs by INFINEON TECHNOLOGIES, INC. was set up on this PCB. They are located opposite to each other, one on the top layer and one on the bottom layer, connected by a via. This way, low stray inductance as in the *HI-LEVEL* case is guaranteed. Around this via, on the inner layers of the PCB, the Rogowski coil is located, measuring the device current of the high-side MOSFET, which is 100 A maximum. Hereby, the shape of the winding was chosen as depicted in figure 1. The horizontal connections are made of copper traces, the vertical connections are buried vias. On the top layer, in the drain path of the high-side MOSFET, a small copper tunnel is located, into which another Rogowski coil can be inserted as a reference measurement. Here, the *CWT Ultra Mini* by POWER ELECTRONIC MEASUREMENTS LTD. [15] with a bandwidth of 20 MHz was used. The DC voltage was chosen to be 20 V. The PCB topology is sketched in figure 3.

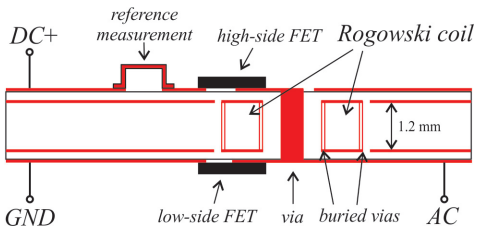

Figure 3: Sketch of the prototype board.

B. Rogowski coil design

From preliminary studies of the presented MOSFET half bridge, the maximum current gradient during switching could be quantified to approximately $1.8\,{}^{\mathrm{A}}/_{\mathrm{ns}}$. According to (3), the choice of $M \approx 4\,\mathrm{nH}$ results in a maximum output voltage of approximately $7.2\,\mathrm{V}$.

Because of the considerations in section II-B, a low number of turns N was chosen, combined with rotational symmetry to enhance measurement accuracy. According to (4), mutual inductance had to be obtained rather by larger coil dimensions than by number of turns. In order to come to an optimal compromise, the concept of an efficiency factor as presented in [10] was introduced, describing the amount of mutual inductance per occupied PCB volume. The effect of only the coil's dimensions on the efficiency factor is visualized in figure 4, which shows a plot of η/N. The red dot indicates the final design.

$$\eta = \frac{M}{\pi(a+d)^2 h} = \frac{\mu_0}{2\pi^2} \cdot \frac{N \log\left(1 + {}^{a}/_{d}\right)}{(a+d)^2} \tag{6}$$

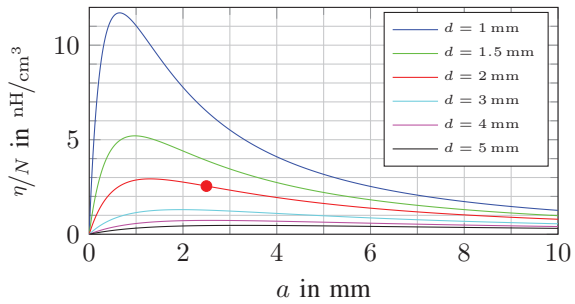

Figure 4: Efficiency factor, describing the amount of mutual inductance per PCB volume and per turn. The final design is indicated by the red dot.

Finally, inductive coupling from external currents should be minimized. As this coil features a low number of turns, it is prone to external fields, so the winding scheme was adopted. In literature, it is discussed that the coil should not only be wound in one direction, but a return wire has to be placed the same way back, so that the coil does not span an area that perpendicular magnetic fields could couple into [5, 12, 13]. This idea was also respected here, but the return wire is a winding as well. This winding scheme is depicted in figure 5 on the left. In PCB layout, each turn of the forth winding is followed by a turn of the return winding, so that they intertwine and minimize the spanned area. In figure 5 on the right, the PCB layout is depicted. The arrows mark the turns of the forth winding, the turns of the return winding are in between.

Given all these considerations, the final design of the PCB Rogowski coil has been made:

- Coil dimensions: $d = 2\,\mathrm{mm}$, $a = 2.5\,\mathrm{mm}$, $h = 1.2\,\mathrm{mm}$
- Number of turns: $N = 20$
- Resulting coil parameters: $M = 3.89\,\mathrm{nH}$, $L_\mathrm{s} = 77.8\,\mathrm{nH}$

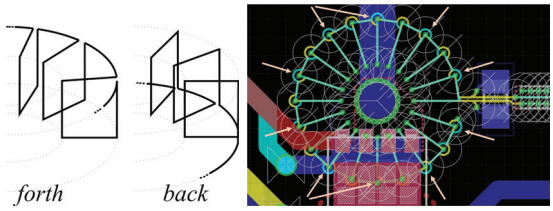

Figure 5: Left: Winding scheme of the PCB Rogowski coil. Right: PCB layout. Arrows mark the turns of the forth winding.

C. The integrator

As according to (3), the coil outputs a voltage proportional to the time derivative of the current, additional integrator circuitry is needed. Integration is done by the use of operational amplifiers. Solely passive integration is, because of its additional attenuation, not realizable, as a Rogowski coil outputs a voltage which is μ_r times lower than the voltage of a conventional current transducer utilizing an iron core. The works of C. R. Hewson, W. F. Ray et al. [4, 6, 8] investigate optimal integrator topologies for Rogowski coils. As they could prove [4, 6] that the conventional inverting integrator has significant disadvantages, the proposed noninverting integrator was chosen in this case. It consists of a passive RC network, performing integration for high frequencies, and an operational amplifier, performing integration for low frequencies. This way, the amplifier can maintain its full bandwidth, as its gain has dropped to unity at the takeover frequency to passive integration. As operational amplifier, the *THS4631* by Texas Instruments, Inc. was chosen. The integrator topology is shown in figure 6.

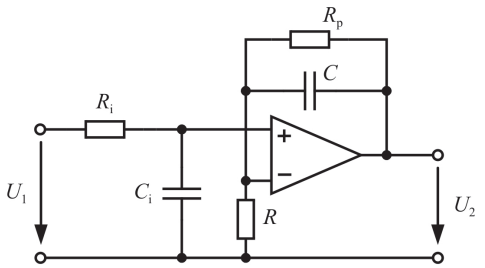

Figure 6: The noninverting integrator topology with a RC lowpass.

IV. Experimental verification

A. Frequency domain analysis

In order to quantify the parasitic elements of the coil model in figure 2, the PCB coil was connected to a 110 MHz impedance analyser. Figure 7 shows the measurement of R_s and L_s in a bandwidth of 100 kHz to 110 MHz:

For low frequencies, the coil's resistance is measured to be $R_\mathrm{s} = 0.876\,\Omega$ and its self-inductance to be $L_\mathrm{s} = 113\,\mathrm{nH}$, which is $45\,\%$ above the expected value. The increase of R_s might be due to the skin effect. At the resonance frequency, the coil would change its characteristics to capacitive behaviour, i.e. negative values for the measured self-inductance. As no

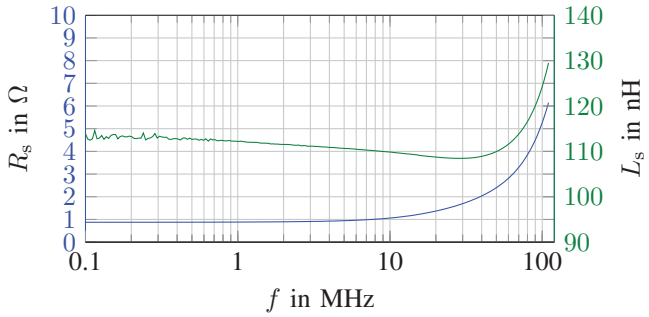

Figure 7: Measurements of the coil impedance.

zero point occurs, it can be supposed that the designed PCB coil has a bandwidth of greater than 110 MHz.

Therefore, the considerations in chapter III-B were overcautious. Instead, a much larger number of turns could have been chosen to produce higher output voltage.

B. Time domain analysis

Afterwards, the PCB Rogowski coil and the integrator were unified and measured in time domain with a non-sinusoidal current waveform created by a double pulse test. It produces a linearly increasing current, intercepted by a short turn-off period. For all experiments, this waveform was left unchanged for better comparability. The maximum current after the first pulse is 25 A. In figure 8, the current measurement of the reference Rogowski coil and the measurement of the PCB Rogowski coil with the proposed integrator are compared.

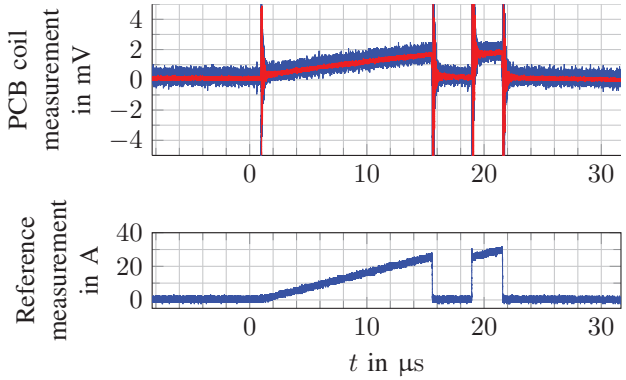

Figure 8: Top: Raw measurement data (blue plot) and 20 MHz-filtered data (red plot). Bottom: Reference measurement.

Apparently, the measurement with the PCB coil very roughly reproduces the current waveform. However, the desired signal is disturbed with a substantial amount of noise and large voltage spikes followed by oscillations. Surprisingly, these even occur at $t \approx 1\,\mu s$, where the current is still zero. It is presumed that a large voltage gradient of the drain to source voltage of the MOSFET injects a current i_{couple} through some parasitic coupling capacitances C_p into the coil, where it causes a voltage drop u_{couple} over the coil's impedance, see figure 9 on the left. Obviously, this system cannot be considered a satisfactory current sensor.

C. The differential Rogowski coil

S. Hain and M.-M. Bakran [14] proposed a promising approach to eliminate capacitive coupling. They wound two coils instead of one on the bearing, using a twisted-pair wire, so that the coils were shaped as similarly as possible. Now receiving two signals, they connected one end of the first coil and the *opposite* end of the second coil to ground, so that the signals created by the current had different polarities, as the two coils now seemed to be wound in opposite directions. As capacitive coupling does not depend on winding direction, the undesired signal components had same polarities. By subtracting the two signals, they cancelled out. This principle is called a *'differential Rogowski coil'*. By grounding the midpoint of the PCB coil at the transition from the forth to the return winding, the differential approach was very easily transferable to this setup.

In figure 9, a simplified model of the single-ended and the differential coil is shown. The green paths mark the direction of capacitive displacement current flow.

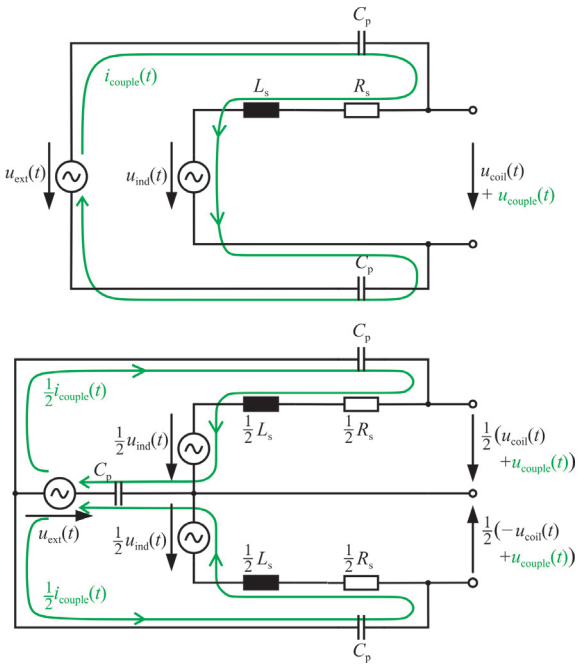

Figure 9: Top: Simplified model of capacitive coupling onto a single-ended Rogowski coil. Bottom: Simplified model of capacitive coupling onto a differential Rogowski coil [14].

As a first test, the two differential branches were measured separately. Figure 10 depicts a 10 A current turn-off. The upper figure shows the drain current (reference measurement) and the drain to source voltage of the MOSFET, the lower figure shows the voltage of the two differential branches. It can be observed that the voltage spike, which is induced by the current transient, appears with different polarity on both branches. However, the subsequent oscillations, which have been disturbing the measurements so far, quickly run in phase so that a subtracting element would reduce their amplitude.

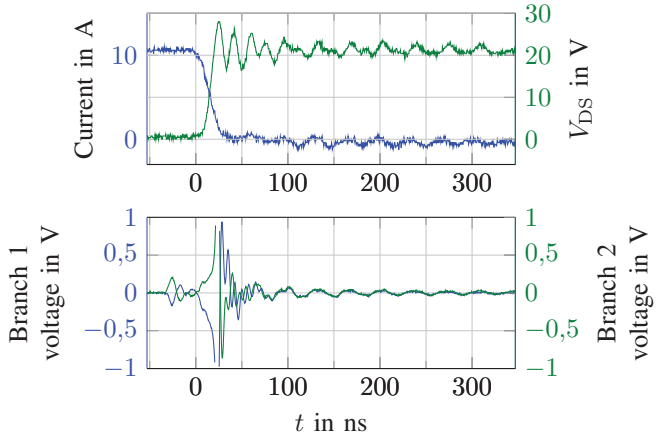

Figure 10: Measurement of the differential coil branches (lower figure) during a 10 A current turn-off (upper figure). Data are 20 MHz-filtered.

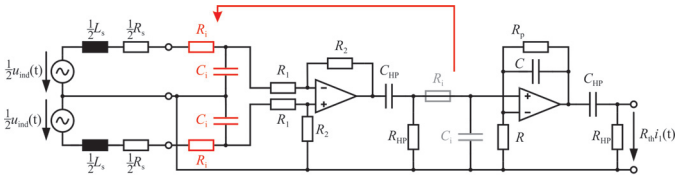

Figure 11: Schematic of the differential Rogowski coil with the *THS4631* subtractor and the split integrator.

As a differential stage, another *THS4631* was configured as a voltage subtractor, as shown in figure 11. By the choice of R_1 and R_2, a differential gain of $K_{\text{diff}} = 100$ was introduced additionally. Such a high gain would cause the amplifier to overdrive when a voltage spike caused by a current turn-off is induced in the coil. Therefore, the integrator topology was split and the passive $R_\text{i}C_\text{i}$ stage was moved in front of the subtractor. This way, C_i buffers the energy of the voltage spike and the amplifier does not overdrive. The measurement results are depicted in figure 12.

Obviously, noise and capacitive disturbances are reduced substantially due to differential measurement and preamplification and the reference current waveform is reproduced quite well. However, if the two differential branches are swapped, which theoretically would not make a difference but a sign, two *different* output signals can be measured (blue and red plot) due to some unknown asymmetries of the system. Possible reasons could be:

- An asymmetry of the coil itself, as each differential branch has only $N/2 = 10$ turns
- Coupling of the coil and the integrator through R_2, which was shown to be unfortunate in some cases [4, 6]
- Incorrect matching of the resistors R_1 and R_2
- The resistors provide false termination to the coil

Except for the coil itself, these possibilities can be eliminated by the use of an instrumentation amplifier. In this case, the *AD8421* by Analog Devices, Inc. with a differential gain of $K_{\text{diff}} = 19$ was used, as shown in figure 13. The

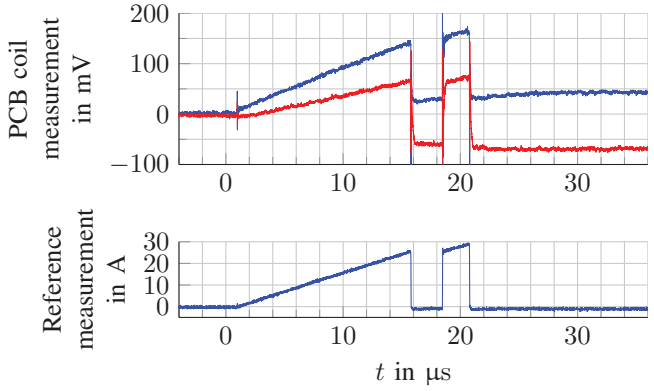

Figure 12: Measurement with the *THS4631* subtractor, $K_{\text{diff}} = 100$ and the split integrator topology.

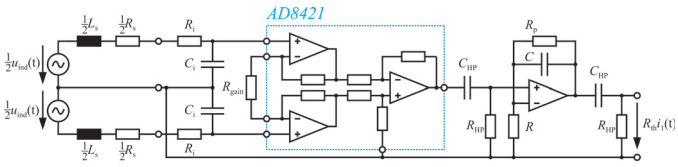

Figure 13: Schematic of the differential Rogowski coil with the *AD8421* instrumentation amplifier and the split integrator.

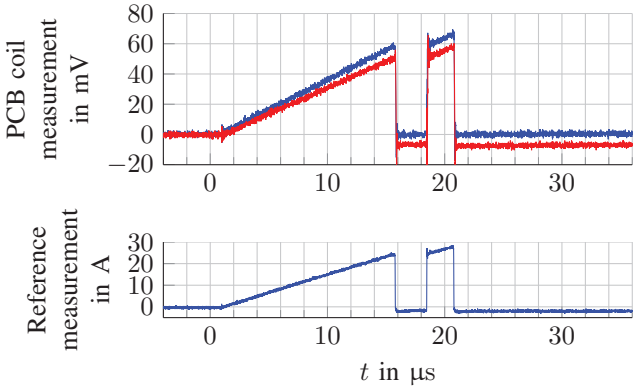

Figure 14: Measurement with the *AD8421* instrumentation amplifier, $K_{\text{diff}} = 19$ and the split integrator topology.

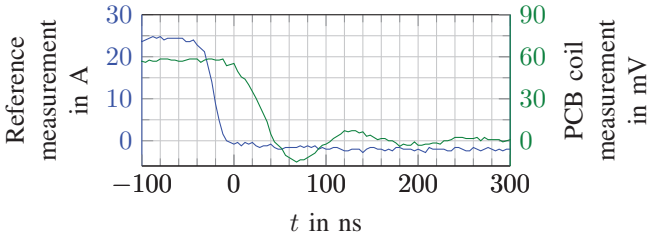

Figure 15: Zoom on current turn-off during a differential measurement with the *AD8421* instrumentation amplifier and $K_{\text{diff}} = 19$.

measured waveforms, which are plotted in figure 14, show very little noise and capacitive disturbances, and the asymmetry between the measurements for different coil polarities is minimized. Additionally, a zoom on the first current turn-off is plotted in figure 15, comparing the dynamics of the reference

measurement and of the PCB coil. Obviously, the whole circuit shows good dynamic performance.

However, the *AD8421* yet constitutes the greatest loss in bandwidth and dynamics in general, as its bandwidth is limited to $20\,\mathrm{MHz}$ for $K_{\mathrm{diff}} \leq 10$ and its slew rate is as low as $35\,{}^{\mathrm{V}}/_{\mu\mathrm{s}}$.

V. Conclusion

In this paper, a current sensor based on the principle of a Rogowski coil has been designed, which should be located inside a PCB near a power semiconductor device. Such a sensor was motivated by the *HI-LEVEL* project, which deals with the integration of power semiconductor devices into a PCB.

The theoretical part of the work especially focused on how to achieve both measurement accuracy and high dynamics. Based on this knowledge, a prototype board has been designed on a 4-layer PCB. It includes a low-inductive MOSFET half bridge and the PCB Rogowski coil, which has been optimized regarding measurement accuracy, dynamics, occupied volume and coupling from external magnetic fields.

Frequency characterization of the PCB coil revealed a bandwidth of greater than $110\,\mathrm{MHz}$, but time domain analysis revealed poor SNR and capacitive disturbances from the high voltage gradients that occur in the MOSFETs. Therefore, the principle of the differential Rogowski coil was researched and applied onto the coil. Single differential measurements showed that the principle works fine with the PCB coil. The differential stage, which first showed significantly asymmetric behaviour regarding the two differential branches, was optimized using an instrumentation amplifier. Elimination of remaining asymmetries would be the main objective to future research. Additionally, all electronics should be optimized regarding bandwidth.

For example, the number of turns should be increased, as the resonance frequency can be reduced. This might have the advantage that measurement accuracy is increased, the coupling from external currents is reduced, the coil symmetry is increased, the output signal is increased and that the effect of different coil terminations can be examined. Maybe even the two differential branches should be implemented without a common mid-point, so that a different grounding would require addition of the two signals instead of subtraction, maximizing the symmetry of the differential stage. At last, it could be examined if a rudimentary shielding of the coil using copper planes and a series of buried vias in a 6-layer PCB could help to divert capacitive displacement currents [7, 8], or if it only would degrade bandwidth.

All in all, one can say that detailed literature research and theoretical work, combined with careful system design, have led to a prototype of a PCB integrated Rogowski coil, which, when operating in differential mode, performs measurements of little noise, good dynamic quality and high immunity to voltage gradients at only a few nH of mutual inductance and only $64\,\mathrm{mm}^2$ of occupied PCB area.

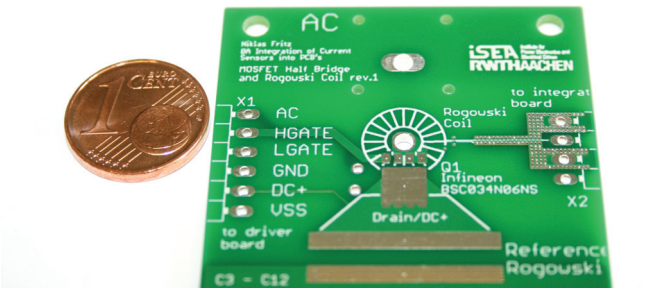

Figure 16: Zoomed view on the designed PCB Rogowski coil.

References

[1] Chattock, A. P. 'On a Magnetic Potentiometer'. In: *Proceedings of the Physical Society of London* 9.1 (1887), pp. 23–26. DOI: 10.1088/1478-7814/9/1/305. URL: http://iopscience.iop.org/1478-7814/9/1/305/.

[2] Rogowski, W. and Steinhaus, W. 'Die Messung der magnetischen Spannung'. In: *Archiv für Elektrotechnik* 1.4 (1912), pp. 141–150. ISSN: 0003-9039. DOI: 10.1007/BF01656479. URL: http://link.springer.com/article/10.1007/BF01656479.

[3] Karrer, N. and Hofer-Noser, P. 'A New Current Measuring Principle for Power Electronic Applications'. In: *The 11th International Symposium on Power Semiconductor Devices and ICs (ISPSD)*. IEEE, 1999, pp. 279–282. DOI: 10.1109/ISPSD.1999.764117.

[4] Ray, W. F. and Davis, R. M. 'High Frequency Improvements in Wide Bandwidth Rogowski Current Transducers'. In: *8th European Conference on Power Electronics and Applications, Lausanne*. EPE Association, Sept. 1999, P.1–P.9. URL: http://www.capturedlightning.org/hot-streamer/teslacoils/Misc/RogowskiCoils-816epe99.pdf.

[5] Karrer, N. and Hofer-Noser, P. 'PCB Rogowski Coils for High di/dt Current Measurement'. In: *IEEE 31st Annual Power Electronics Specialists Conference (PESC)*. Vol. 3. IEEE, 2000, pp. 1296–1301. DOI: 10.1109/PESC.2000.880497.

[6] Ray, W. F. and Hewson, C. R. 'High Performance Rogowski Current Transducers'. In: *Conference Record of the 2000 IEEE Industry Applications Conference*. Vol. 5. IEEE, 2000, pp. 3083–3090. DOI: 10.1109/IAS.2000.882606.

[7] Oates, C. D. M., Burnett, A. J., and James, C. 'The Design of High Performance Rogowski Coils'. In: *International Conference on Power Electronics, Machines and Drives*. IEEE, June 2002, pp. 568–573. DOI: 10.1049/cp:20020179.

[8] Hewson, C. R. and Ray, W. F. 'The Effect of Electrostatic Screening of Rogowski Coils Designed for Wide-Bandwidth Current Measurement in Power Electronic Applications'. In: *IEEE 35th Annual Power Electronics Specialists Conference (PESC)*. Vol. 2. IEEE, June 2004, pp. 1143–1148. DOI: 10.1109/PESC.2004.1355583.

[9] Wang, B., Wang, D., and Wu, W. 'A Rogowski Coil Current Transducer Designed for Wide Bandwidth Current Pulse Measurement'. In: *IEEE 6th International Power Electronics and Motion Control Conference (IPEMC)*. IEEE, May 2009, pp. 1246–1249. DOI: 10.1109/IPEMC.2009.5157575.

[10] Li, Y., Guo, Y., Long, Y., Yao, C., Mi, Y., and Wu, J. 'Novel Lightning Current Sensor Based on Printed Circuit Board Rogowski Coil'. In: *International Conference on High Voltage Engineering and Application (ICHVE)*. IEEE, Sept. 2012, pp. 334–338. DOI: 10.1109/ICHVE.2012.6357121.

[11] Neeb, C., Ostmann, A., Hofmann, T., Boettcher, L., Manessis, D., and Lang, K. 'Embedded Power Electronics for Automotive Applications'. In: *7th International Microsystems, Packaging, Assembly and Circuits Technology Conference (IMPACT)*. IEEE, Oct. 2012, pp. 163–166. DOI: 10.1109/IMPACT.2012.6420235.

[12] Tao, T., Zhao, Z., Ma, W., and Pan, Q. 'Precise Mutual-Inductance Analysis of a Novel Clasp Rogowski Coil with Symmetrical Double-Printed Imprints'. In: *Sixth International Conference on Electromagnetic Field Problems and Applications (ICEF)*. IEEE, June 2012, pp. 1–4. DOI: 10.1109/ICEF.2012.6310421.

[13] Gerber, D., Guillod, T., Leutwyler, R., and Biela, J. 'Gate Unit With Improved Short-Circuit Detection and Turn-Off Capability for 4.5-kV Press-Pack IGBTs Operated at 4-kA Pulse Current'. In: *IEEE Transactions on Plasma Science* 41.10 (Oct. 2013), pp. 2641–2648. DOI: 10.1109/TPS.2013.2280379.

[14] Hain, S. and Bakran, M.-M. 'New Rogowski Coil Design with a High dv/dt Immunity and High Bandwidth'. In: *15th European Conference on Power Electronics and Applications (EPE)*. IEEE, Sept. 2013, pp. 1–10. DOI: 10.1109/EPE.2013.6631855.

[15] Power Electronic Measurements Ltd. *PEM New CWT Ultra Mini Current Probe*. Aug. 2013. URL: http://www.pemuk.com/products/cwt-current-probe/cwt-ultra-mini.aspx.

[16] Neeb, C., Boettcher, L., Conrad, M., and De Doncker, R. W. 'Innovative and Reliable Power Modules: A Future Trend and Evolution of Technologies'. In: *IEEE Industrial Electronics Magazine* 8.3 (Sept. 2014), pp. 6–16. DOI: 10.1109/MIE.2014.2304313.